

corded for the major portion of the distribution curve can be conservatively interpreted as contributing limited support to the K.U. theory.

ACKNOWLEDGMENTS

The writer wishes to express his sincere appreciation for the inspiration to begin the above investigation and the encouragement to carry it to completion which was given by Professor Robley D. Evans, under whose direction the work was done.

It is also a pleasure to acknowledge the cooperation of Professor A. F. Koyarik of Yale University who was kind enough to prepare a thorium B source on two occasions. This source was used for the calibration of the magnetic field and determination of the efficiency of the spectrometer.

The radium E sources were obtained from Dr. L. R. Hafstad of the Department of Terrestrial Magnetism, Carnegie Institution of Washington, as well as from Professor J. A. Bearden and Dr. W. R. Kanne of the Johns Hopkins University.

It was only the continued courtesy of those just named that made it possible to study the radium E beta-ray spectrum under the various conditions reported in this paper.

For data concerning the design and operation of the spectrometer as well as for information concerning the Fermi and Konopinski-Uhlenbeck theories the writer is also deeply indebted to Dr. L. I. Schiff.

A like debt of gratitude is owed to Dr. N. S. Gingrich and Dr. E. J. Schrepf for advice on the electrical circuits used in the counting apparatus.

AUGUST 15, 1937

PHYSICAL REVIEW

VOLUME 52

Extreme Ultraviolet Series in Cr VI, Mn VII and Fe VIII¹

P. GERALD KRUGER AND S. G. WEISSBERG
University of Illinois, Urbana, Illinois

(Received June 14, 1937)

Lines in the extreme ultraviolet region involving the $3d^2D$, $4p^2P$, $5s^2S$, $6s^2S$, and several nf^2F terms have been identified in the spectra of Mn VII and Fe VIII. In Cr VI the first member of the $3d^2D-nf^2F$ series has been found. These spectra have been photographed with a twenty-one foot grazing incidence vacuum spectrograph. Identification was facilitated by the use of constant second difference displaced frequency diagrams.

THE spectra of highly ionized chromium, manganese and iron have been photographed in the extreme ultraviolet with a twenty-one foot grazing incidence vacuum spectrograph. The instrument and source of power have been described in previous reports.^{2, 3}

Heretofore the identification of the extreme ultraviolet spectra of isoelectronic ions by the use of the constant second difference law, has been greatly facilitated by the fact that the lines involved were among the very strongest in the region. However, when an attempt was made to extend the K I—Cr VI isoelectronic sequence to Mn VII, an extrapolation of the displaced fre-

quency diagram (see Fig. 1) for the resonance multiplet $3d^2D_{3/2, 5/2}-4p^2P_{1/2, 3/2}$ led into a thickly populated region, with no prominent lines. This was in contrast to the appearance, on our plates, of the very strong $3d^2D_{3/2, 5/2}-4p^2P_{1/2, 3/2}$ multiplets in V V and Cr VI.⁴ That Mn VII might not be excited would indeed be curious, since spectra both from Mn VI and Mn VIII have been identified on the same plates, and lines from both of these ions are intense. One must conclude, therefore, that the above multiplet is among the lines of intermediate intensity in Mn VII.

From the identification of the multiplet $4s^2S_{1/2}-4p^2P_{1/2, 3/2}$, Gibbs and White had already found the fine structure interval in the

¹ Preliminary report given by P. G. Kruger and S. G. Weissberg, *Phys. Rev.* **49**, 873A (1936).

² P. G. Kruger, *Rev. Sci. Inst.* **4**, 128 (1933).

³ P. G. Kruger and W. E. Shoupp, *Phys. Rev.* **46**, 124 (1934).

⁴ Previously reported by R. C. Gibbs and H. E. White, *Proc. Nat. Acad. Sci.* **12**, 598, 675 (1926).

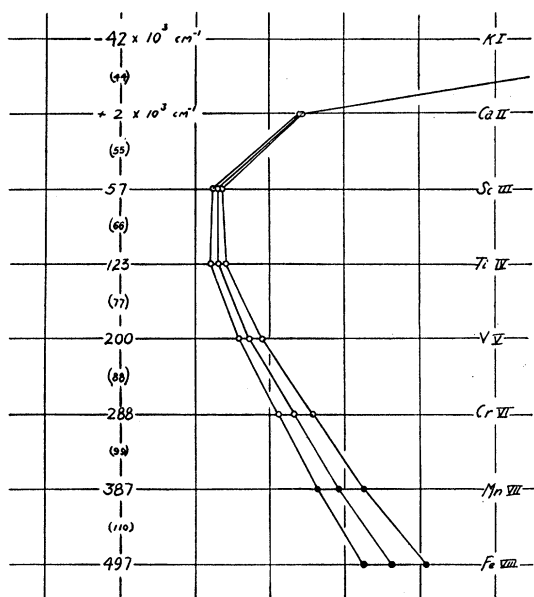


FIG. 1. Displaced frequency diagram with constant second difference of $11,000 \text{ cm}^{-1}$ for resonance multiplet $3d^2D_{3/2, 5/2} - 4p^2P_{1/2, 3/2}$. Horizontal scale: 1 div. = 4000 cm^{-1} .

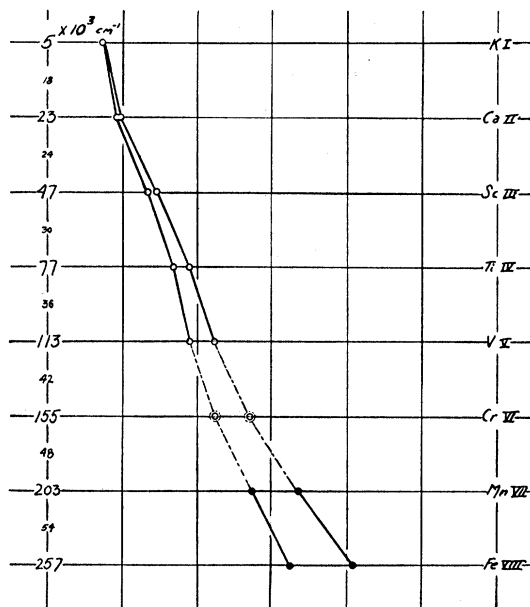


FIG. 2. Displaced frequency diagram with constant second difference of 6000 cm^{-1} for $4p^2P_{1/2, 3/2} - 5s^2S_{1/2}$. Horizontal scale: 1 div. = 4000 cm^{-1} .

$4p^2P$ term in Mn VII to be 2464.7 cm^{-1} . This interval was verified by us with the discovery of the $4p^2P_{1/2, 3/2} - 5s^2S_{1/2}$ and $4p^2P_{1/2, 3/2} - 6s^2S_{1/2}$ multiplets, their approximate location being predicted with the use of displaced frequency diagrams. (See Figs. 2, 3.)

An approximate value (1340 cm^{-1}) of the $3d^2D$ fine structure interval was found graphically by extrapolating a σ vs. Z graph, where σ and Z are related by the regular doublet law, $\Delta\nu = R\alpha^2(Z - \sigma)^4/n^3l(l+1)$. The resonance multiplet selected yielded 2467 cm^{-1} for the 2P interval and 1344 cm^{-1} for the 2D interval.

On one of our Mn plates, a series of four pairs of lines with nearly the same frequency difference appeared. These were fitted to the formula

$$\nu_m = 961,517 - 49R/(m - 0.092)^2,$$

where $m = 6, 7, 8, 9$. (This formula is for the lower ν of the pairs.) The close fit of this limit with the limit predicted for the $3d^2D$ terms by the use of a Moseley diagram, and the similarity of the frequency intervals ($1341, 1323, 1353, 1355 \text{ cm}^{-1}$) to the $3d^2D$ interval of 1344 cm^{-1} suggested strongly that the series had $3d^2D$ as the common lower state. There were two possi-

bilities, namely a $3d^2D - nf^2F$ and a $3d^2D - np^2P$ series. Members of the 2P series would normally consist of three lines with relative intensities (ν increasing) of 5, 9, 1, and with the

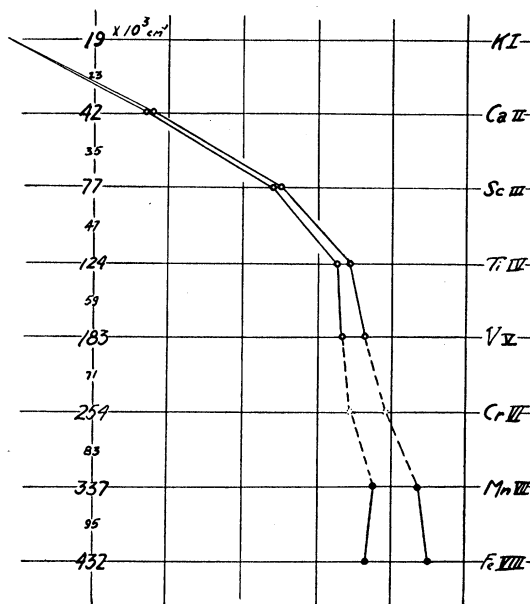


FIG. 3. Displaced frequency diagram with constant second difference of $12,000 \text{ cm}^{-1}$ for $4p^2P_{1/2, 3/2} - 6s^2S_{1/2}$. Horizontal scale: 1 div. = 4000 cm^{-1} .

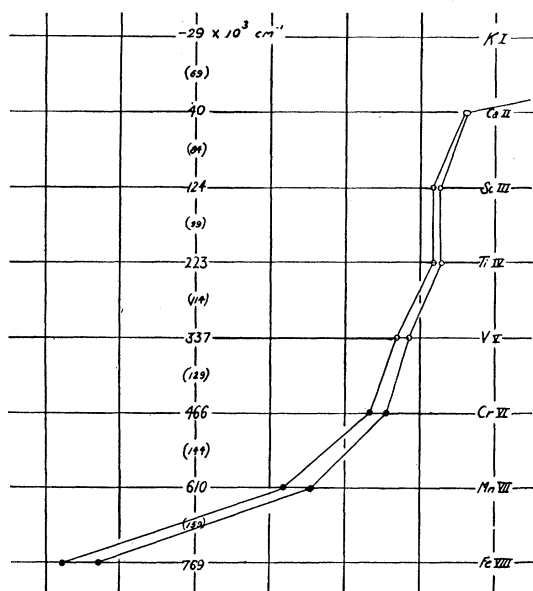


FIG. 4. Displaced frequency diagram with constant second difference of $15,000 \text{ cm}^{-1}$ for first members of the $3d^2D_{3/2, 5/2} - nf^2F_{5/2, 7/2}$ series. Horizontal scale: 1 div. = 4000 cm^{-1} .

2P interval nearly twice the 2D interval. Members of the 2F series, on the other hand, would consist of three lines, with relative intensities (ν increasing) of 5, 100, 70, but with the 2F interval very much smaller than the 2D interval. Hence, if only two lines appeared, members of the 2P series would show the line of shorter wave-length to be the more intense, whereas the opposite would be the case for a 2F series. In the series at hand, the more intense line in each pair is of longer wave-length. This points to identification of the series as a $3d^2D - nf^2F$ series.

The term values were calculated for this 2F series by fitting the lines $\nu = 806,419$, $847,515$, and $874,181 \text{ cm}^{-1}$ to a Ritz-Rydberg formula given by

$$\nu_m = A - Z^2R / (m + \mu + \alpha T_m)^2 = A - T_m,$$

where A is the series limit, m is an integer, $\mu = -0.1370$ and $\alpha = 2.68 \times 10^{-7}$, and T_m is the term value.

Once these terms were established, and the trend of the variation of the quantum defects known, the identification of the $3d^2D - 4f^2F$ and $3d^2D - 5f^2F$ lines offered no difficulty. Identification of the first member was assisted somewhat by the displaced frequency diagram (Fig. 4).

TABLE I. Observed lines and transitions.

TRANSITION	$\lambda(\text{Å})$	INT.	$\nu(\text{cm}^{-1})$	$\Delta\nu(\text{cm}^{-1})$
Mn VII				
$4p^2P_{3/2} - 5s^2S_{1/2}$	467.662	30	213830	2450
$4p^2P_{1/2} - 5s^2S_{1/2}$	462.363	15	216280	
$4p^2P_{3/2} - 6s^2S_{1/2}$	284.059	10	352040	2450
$4p^2P_{1/2} - 6s^2S_{1/2}$	282.095	3	354490	
$3d^2D_{3/2} - 4p^2P_{1/2}$	251.479	1	397647	2467
$3d^2D_{5/2} - 4p^2P_{3/2}$	250.771	4	398770	
$3d^2D_{3/2} - 4p^2P_{3/2}$	249.929	2	400114	1344
$3d^2D_{5/2} - 4f^2F_{5/2}$	162.707	30	614602	
$3d^2D_{5/2} - 4f^2F_{7/2}$	162.667	60	614753	151
$3d^2D_{3/2} - 4f^2F_{5/2}$	162.349	80	615957	
$3d^2D_{5/2} - 5f^2F_{5/2}$	135.425	2	738416	174
$3d^2D_{5/2} - 5f^2F_{7/2}$	135.393	25	738590	
$3d^2D_{3/2} - 5f^2F_{5/2}$	135.177	20	739771	1355
$3d^2D_{5/2} - 6f^2F_{7/2}$	124.005	15	806419	
$3d^2D_{3/2} - 6f^2F_{5/2}$	123.799	10	807760	1341
$3d^2D_{5/2} - 7f^2F_{7/2}$	117.992	5	847515	
$3d^2D_{3/2} - 7f^2F_{5/2}$	117.808	3	848838	1323
$3d^2D_{5/2} - 8f^2F_{7/2}$	114.393	2	874181	
$3d^2D_{3/2} - 8f^2F_{5/2}$	114.216	1	875534	1353
$3d^2D_{5/2} - 9f^2F_{7/2}$	112.260	1	892387	
$3d^2D_{3/2} - 9f^2F_{5/2}$	111.889	0	893742	1355
Cr VI				
$3d^2D - 4f^2F$	210.288	6	475312	
$3d^2D - 4f^2F$	209.978	4	476240	

The complete list of wave-lengths identified in Mn VII is given in Table I. Two new lines have been assigned to Cr VI, namely the two strong lines of the $3d^2D - 4f^2F$ transitions.

The analysis of the Fe VIII lines presented the same problems met in Mn VII with the addition that the $4p^2P$ fine structure interval was unknown. Reliance was placed on the screening constant extrapolation for an approximate value of the $4p^2P\Delta\nu$. The $^2P - ^2S$ lines were easily

TABLE II. Observed lines and transitions. Fe VIII.

TRANSITION	$\lambda(\text{Å})$	INT.	$\nu(\text{cm}^{-1})$	$\Delta\nu$
$4p^2P_{3/2} - 5s^2S_{1/2}$	370.432	10	269955	3364
$4p^2P_{1/2} - 5s^2S_{1/2}$	365.873	4	273319	
$4p^2P_{3/2} - 6s^2S_{1/2}$	223.870	4	446688	3379
$4p^2P_{1/2} - 6s^2S_{1/2}$	222.189	4	450067	
$3d^2D_{3/2} - 4p^2P_{1/2}$	196.046	15	510084	3363
$3d^2D_{5/2} - 4p^2P_{3/2}$	195.476	20	511572	
$3d^2D_{3/2} - 4p^2P_{3/2}$	194.762	5	513447	1875
$3d^2D_{5/2} - 4f^2F_{7/2}$	131.242	9	761951	
$3d^2D_{3/2} - 4f^2F_{5/2}$	130.939	8	763714	1763
$3d^2D_{5/2} - 5f^2F_{7/2}$	108.083	8	925214	
$3d^2D_{3/2} - 5f^2F_{5/2}$	107.872	8	927024	1810
$3d^2D_{5/2} - 6f^2F_{7/2}$	98.522	4	1015002	
$3d^2D_{3/2} - 6f^2F_{5/2}$	98.345	4	1016828	1826
$3d^2D_{5/2} - 7f^2F_{7/2}$	93.374*	3	1071000	
$3d^2D_{3/2} - 7f^2F_{5/2}$	93.217*	3	1072765	1846

* Absolute values of λ probably in error by 0.01Å.

TABLE III. Term values and effective quantum numbers.

Mn VII							
	$n=3$	4	5	6	7	8	9
$^2S_{1/2}$		643267 2.8912	348067 3.9304	209857 5.0618			
$^2P_{1/2}$		564354 3.0867					
$^2P_{3/2}$		561889 3.0935					
$^2D_{3/2}$	962001						
$^2D_{5/2}$	2.3642 960646 2.3658						
$^2F_{5/2}$		346044 3.9419	222230 4.9190				
$^2F_{7/2}$		345893 3.9430	222056 4.9209	154241 5.9044	113163 6.8932	86467 7.8859	68259 8.8755

Fe VIII				
	$n=3$	4	5	6
$^2S_{1/2}$			435958 4.0137	259225 5.2051
$^2P_{1/2}$		709276 3.1467		
$^2P_{3/2}$		705913 3.1542		
$^2D_{3/2}$	1219360			
$^2D_{5/2}$	2.3999 1217485 2.4018			
$^2F_{5/2}$		455646 3.9260	292336 4.9015	202532 5.8887
$^2F_{7/2}$		455539 3.9264	292276 4.9020	202483 5.8894

found with the aid of the displaced frequency diagrams (Fig. 2). The $3d\ ^2D$ splitting was then obtained from the $^2D-^2F$ series. This permitted the definite location of the resonance lines $3d\ ^2D-4p\ ^2P$. The complete list of wave-lengths of Fe VIII is given in Table II.

Term values and effective quantum numbers are listed in Table III, and the ionization potentials for the entire sequence are shown in Table IV. The value $526,006\text{ cm}^{-1}$ for the $3d\ ^2D$ term in V V is our estimate based on the data of Gibbs and White.⁵ This results from fitting a

⁵ Bacher and Goudsmit, *Atomic Energy States*.

TABLE IV. Ionization potentials in the isoelectronic sequence K I—Co IX.*

ION	$3d\ ^2D_{3/2}$ cm^{-1}	IONIZATION POTENTIAL VOLTS	FIRST DIFFERENCE VOLTS	SECOND DIFFERENCE VOLTS
K I	13470.26	1.6618		
Ca II	82097.8	10.1280	8.4662	6.0404
Sc III	199693	24.6346	14.5066	3.84
Ti IV	348433	42.9845	18.3499	3.56
V V	526006	64.891	21.9065	(3.37)
Cr VI	(730940)	(90.17)	(25.279)	(3.23)
Mn VII	962001	118.677	(28.507)	(3.24)
Fe VIII	1219360	150.427	31.750	(3.22)
Co IX	(1503000)	(185.4)	(34.97)	

* Values in parentheses are estimated from a Moseley diagram. The value for V V has been recalculated from data of Gibbs and White, *Phys. Rev.* **33**, 157 (1929).

Ritz-Rydberg term formula to the 2S terms, as was done by Russell and Lang with Ti IV.⁶ Our estimate is likely to be slightly too deep. This statement is based on the fact that a limit calculation from the 2S terms in Mn VII and Fe VIII leads to a value which is too deep as compared to the more accurate calculation based on the third, fourth, and fifth members of the 2F series in Mn VII and the second, third, and fourth members of the 2F series in Fe VIII.

The ionization potentials in the sequence increase with a nearly constant second difference. Heretofore short range extrapolations of the ionization potential have been made by assuming a constant second difference. This practice is supported by the results of exact series calculations made possible by the identification of several members of the 2F series.

⁶ A. N. Russell and R. J. Lang, *Acous. J.* **66**, 13 (1927).